A Comparative Experimental and Theoretical Study between Heteroarm Star and Diblock Copolymers in the Microphase Separated State

Valérie Grayer, Elena E. Dormidontova,† and Georges Hadziioannou*

Department of Polymer Chemistry and Materials Science Centre, University of Groningen, Nijenborgh 4, 9747 AG Groningen, The Netherlands

Constantinos Tsitsilianis*

Department of Chemical Engineering, University of Patras and Institute of Chemical Engineering and High-Temperature Chemical Processes, ICE/HT-FORT, P.O. Box 1414, 26500 Patras, Greece

Received February 18, 2000; Revised Manuscript Received June 22, 2000

ABSTRACT: A pronounced difference in the behavior of heteroarm star copolymers from the conventional diblock copolymers is analyzed theoretically and experimentally on the example of symmetric polystyrene-poly(2-vinylpyridine) (PS_6P2VP_6) star block copolymer melts. Microphase separation of PS_6P2VP_6 stars with volume fraction of PS varying from 0.30 to 0.75 is studied using transmission electron microscopy (TEM). The observed (lamellar, cylindrical and undefined "bicontinuous-like") structures often turned out to be different from that expected for the corresponding diblock copolymers. The dependence of the long period of lamellar structures of heteroarm star block copolymers on block length is found to deviate in a systematic way from $N^{2/3}$ law (known for diblock copolymers), especially for the stars of high functionality. The theoretical model proposed to describe an extra-stretching of star block copolymers near the lamellar interface is found to be successful in prediction of block length and star functionality dependence of the lamellar period as it agrees remarkably well with the present and other available experimental data for both symmetric and asymmetric heteroarm star block copolymers.

1. Introduction

During the past decade, improvements in "living" polymerization techniques have made possible the synthesis of well-defined block copolymers as well as of novel nonlinear copolymers such as simple graft, star block, and heteroarm star copolymers.[1−14]

In the present study, we focus our attention on A_nB_n heteroarm star copolymers, which are star-shaped molecules constituted of a central core bearing arms of pure polymer A and pure polymer B (Figure 1).[15] Like diblock copolymers, these polymeric species undergo microphase separation either in solution where micelles can be formed[7,16−19] or in the solid state.[12,20−32] On the other hand, the difference in architecture between star and linear copolymers results naturally in much slower phase separation kinetics and in modification of the equilibrium states. Relaxation processes, phase behavior, and ordering of the microdomains formed by star copolymers are all properties influenced by the architecture of the molecules, in particular by the functionality (total number of arms) of the stars.

Few theoretical studies deal with the solid-state phase behavior of heteroarm star copolymers.[33−35] Phase diagrams of graft, $(AB)_n$ star, and A_nB_n heteroarm star copolymers have been calculated by Olvera de la Cruz et al.[33] in the weak segregation limit. For A_nB_n type copolymers, they predicted a symmetrical phase diagram with a critical point at $\phi = 0.5$ and $\chi N_0 = 10.5$, independent of n (where ϕ is the relative volume fraction of one of the components and N_0 is the total number of statistical segments of one A arm plus one B arm). The general features of the phase diagram are very similar to the phase diagram of diblock copolymers. Milner[34] has treated the problem of heteroarm star copolymers in the strong segregation limit introducing a parameter $\epsilon = (n_A/n_B)(l_A/l_B)^{1/2}$ (where n_i is the number of arms of type i = A or B and l_i is given by V_i/R_{gi}^2 where V_i and R_{gi} are the volume and the radius of gyration of one i block, respectively). The parameter ϵ reflects the architectural and conformational asymmetry of the molecules. For stars composed of an equal number of arms of the two polymers ($n_A = n_B$) with similar conformational properties ($l_A = l_B$), $\epsilon \approx 1$ and the phase diagram is identical to that of diblock copolymers.

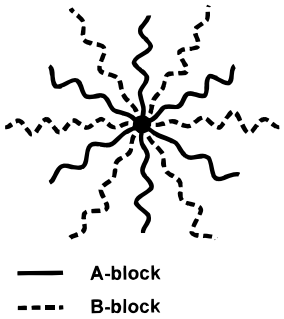

Figure 1. Schematic representation of an heteroarm star copolymer of A_nB_n type.

Most experimental studies regarding the morphology of heteroarm star copolymers are concerned with samples of low functionality (i.e., total number of arms)[30,36] and of asymmetric architecture ($n_A \neq n_B$).[22,25,26,29,32] Pochan et al.[25,26] studied the phase behavior of a series of polyisoprene (PI)/polystyrene (PS) simple graft copolymers noted I_2S. They found a good agreement with the prediction of Milner's model for asymmetric stars in the

† Present address: Department of Chemical Engineering and Material Science, University of Minnesota, 151 Amundson Hall, 421 Washington Ave. S.E.; Minneapolis, MN 55455

10.1021/ma000311u CCC: $19.00
Published on Web 08/03/2000

Table 1. Molecular Characteristics of Polystyrene/Poly(2-vinylpyridine) Heteroarm Star Copolymers

sample[a]	$M_w \times 10^{-4}$ PSarm	M_w/M_n PSarm (GPC)	$M_w \times 10^{-5}$ PS_n	$M_w \times 10^{-5}$ PS_nP2VP_n	W_{P2VP} (%) (NMR)	$M_w \times 10^{-4}$ P2VParm[b]	n[c]
167_6-148_6	2.0	1.15	1.54	2.49	44	1.6 (1.4)	6.9
167_6-282_6	2.0	1.15	1.54	4.39	60	3.9 (4.1)	6.9
167_6-365_6	2.0	1.15	1.54	5.44	66	5.3 (5.9)	6.9
205_6-240_6	2.3	1.08	1.50	3.29	53	2.8 (2.85)	6.3
180_6-65_6	2.3	1.23	1.56	2.12	24	0.85 (0.9)	6.1

[a] The names of the samples are given following the notation: $N(\text{PSarm})_n - N(\text{P2Vparm})_n$, where N(P2Vparm) is calculated by the formula: $N(\text{P2VParm}) = \{M_n(\text{PSarm}) + m_{DVB}[\text{DVB}]/[\text{LE}]\}W_{P2VP}/(1 - W_{P2VP})m_{2VP}$. [b] As calculated from NMR data, using the formula: $M_w(\text{P2VParm}) = M_w(PS_nP2VP_n)W_{P2VP}/n$. Values in parentheses have been calculated from LS data using the formula $M_w(\text{P2VParm}) = [M_w(PS_nP2VP_n) - M_w(PS_n)]/n$. [c] Average functionality: $n = M_w(PS_n)/\{M_w(\text{PSarm}) + m_{DVB}\{\text{DVB}\}/\{\text{LE}\}\}$ where [DVB]/[LE] is the divinylbenzene per living ends mole ratio.

strong segregation limit. As expected, they observed that the extra crowding of the polyisoprene arms partially prevents them to be on the concave side of the interface. As a result, the whole phase diagram shifts toward the higher volume fractions of PS. Tselikas et al.[27] studied the morphology of series of S_2I, I_2S, and I_3S heteroarm star copolymers. They also found a shift in the phase diagram toward higher volume fraction of the single block, but with some discrepancies with Milner's model, which they attribute to multiple domain effects. Very recently, the phase behavior of three highly asymmetrical samples of type I_5S was reported by Beyer et al.[32] Two of their samples exhibit a lamellar ordering in the region where cylinders would be expected.[34] Combining these observations with the results of the earlier studies over three- and four-arm polystyrene/polyisoprene heteroarm star copolymers, they conclude that, in general, Milner's theory overestimates the shift in the phase diagram due to architectural and conformational asymmetry. They note that the discrepancy between the experimental results and the theory increases with increasing ϵ. All these studies indicate that a better understanding of monomer interactions and blocks conformation of heteroarm star copolymers near the interface is required. One attempt in this direction was undertaken by Beyer et al.[28] They reported on morphologies of star copolymers having eight polyisoprene and eight polystyrene arms originating from a carbonsilane dendrimer. They found that the samples of the relative volume fractions of $\phi \sim 0.4-0.5$, form stable lamellar morphologies. For these PS_8PI_8 samples and the S_2I, I_2S, and I_3S samples mentioned above, they studied the scaling dependence of a dimensionless area per junction, $AN^{2/3}/R_g^2$ (where A is the area per molecule at the interface deduced from the lamellar period, N is the total number of statistical segments and R_g^2 is the unperturbed mean square radius of gyration of the star molecule), on the functionality of the stars, f. With arguments based on Alexander−de Gennes theory, they predicted a power law with an exponent equal to one, i.e., $AN^{2/3}/R_g^2 \sim f$. However, this prediction does not seem to fit the experimental data well. Indeed, the best fit of the experimental data for small values of f ($1 < f \leq 4$) gives an exponent of ~0.8, while for higher values of f, the corresponding exponent is higher than 1.2.

The objective of this paper is to investigate in more detail the behavior of A_nB_n heteroarm star copolymers. Our approach is 2-fold. First, we study the phase behavior of a series of polystyrene/poly(2-vinylpyridine) (P2VP) heteroarm star copolymers of type PS_nP2VP_n presenting a relatively high functionality of 12. By keeping the length of the PS arms nearly constant while varying the length of the P2VP arms, we cover a composition range from $\phi_{PS} = 0.30$ to 0.75. Second, we analyze the influence of the star functionality on the lamellar ordering by examining the period of lamellar structures formed by different heteroarm copolymers. A theoretical model is suggested (using the analogy between the star polymers and polymer micelles) to predict the scaling law of the lamellar period on the functionality $f_I \equiv n$ and the length (degree of polymerization) of the blocks N_I, where I = A or B. We find an excellent agreement between the prediction of our model and data obtained for our PS_6P2VP_6 samples and the PS_8PI_8 stars studied by Beyer et al.[28] Extension of our model to asymmetrical low functionality samples studied in refs 14, 16, and 20 also proves to be successful. Introducing a correction accounting for the lower degree of stretching of the single block, we find that the size of the lamellae layer formed by the other blocks follows the same scaling law as it does for the symmetrical high functionality stars.

2. Experimental Section

2.1. Synthesis and Characterization. The PS_nP2VP_n heteroarm star copolymers were prepared by sequential anionic "living" copolymerization using a three-step procedure.[37] First, PS arms are synthesized. Then they are joined together by reacting the living PS chains with a small amount of divinylbenzene (DVB). A star-shaped polystyrene is formed, bearing on its poly(divinylbenzene) core a number of active sites equal to the number of PS arms attached to it. Finally, P2VP arms are grown from the cores, forming the final product, which is a star polymer with equal number of PS and P2VP arms originating from a tight poly(divinylbenzene) core. This procedure provides symmetry on the number of arms of the two species and allows the synthesis in the same reaction of a series of heteroarm star copolymers by varying only the length of the second generation of arms, i.e., the P2VP blocks. Details of the synthesis procedure are reported elsewhere.[37]

All the samples were freed from linear PS precursor and characterized by means of light scattering (LS), nuclear magnetic resonance of the proton (^{1}H NMR), and gel permeation chromatography (GPC). Their molecular characteristics are given in Table 1. We should indicate here that a slight polydispersity in the number of arms can be present due to the random character of the polymerization of the DVB forming the hart of the star polymer. The functionality of the stars is therefore given as a mean value. Nevertheless, the synthetic procedure ensures the constitution of an equal number of arms of PS and P2VP, which is a far more important factor for the phase behavior of the material.[38]

2.2. Film Preparation. Thin films of the different copolymers were cast by deposition of droplets of diluted solutions (~0.1 wt %) in chloroform on a smooth epoxy substrates covered with an 80 nm layer of gold. The films obtained after evaporation of the solvent at room temperature were a few hundreds of nanometers thick. They were allowed to dry in a vacuum and subsequently annealed for 17 h at 160 °C, i.e., well above the glass transition temperature of PS and P2VP.

Table 2. Morphological Characteristics of the PS_nP2VP_n Diblock and Heteroarm Star Copolymers

sample	f	χN_0[a]	ϕ_{PS}[b]	morphology	L_{exp} (nm)
167_1-257_1	2.0	47	0.44	LAM	27
180_6-65_6	12.2	27	0.75 (0.74)[c]	CYL	20
167_6-148_6	13.8	35	0.58 (0.61)[c]	LAM	27
205_6-240_6	12.6	49	0.48 (0.48)[c]	LAM	35
167_6-282_6	13.8	49	0.36 (0.35)[c]	LAM	37
167_6-365_6	13.8	59	0.30 (0.28)[c]	BIC	40

[a] $N_0 = N(\text{PSarm}) + N(\text{P2VParm})$ and $\chi = 0.11$ from ref 42. [b] $\phi_{PS} = [M_w(\text{PSarm})/d_{PS}]/\{[M_w(\text{PSarm})/d_{PS}] + [M_w(\text{P2VParm})/d_{P2VP}]\}$ values in parentheses have been obtained using M_w(P2VParm) values in parentheses of Table 1.

Cross-sectioning of the as-cast and annealed films was achieved using ultramicrotomy. The thin sections were picked up on TEM grids preliminarily covered with an organic support film and coated with carbon. The specimens were submitted for 1 h to iodine vapors in order to stain the P2VP-rich regions. Cross-sectional views of the films were recorded using a JEOL 1200-EX transmission electron microscope operating at 100 kV.

3. Results and Discussion

We have synthesized five symmetrical PS_nP2VP_n star copolymers with a mean overall functionality of 12. The samples 167_6-148_6, 167_6-282_6, and 167_6-365_6 were produced from the same reaction batch. The volume fractions of PS determined by NMR are 0.58, 0.36, and 0.30, respectively. Two other samples 180_6-65_6 and 205_6-240_6 with volume fractions of PS equal to 0.75 and 0.48, respectively, complete the series. Those latter samples were synthesized in separated reaction batches but have characteristics similar to those of the former three samples (i.e., the average number of arms and the molecular weight of the PS linear precursor are nearly identical). This series covers the interval from $\phi_{PS} = 0.30$ to 0.75 (Table 2). We also synthesized and studied a PS−P2VP diblock copolymer with a volume fraction of PS equal to 0.44. This diblock copolymer, denoted as 167_1-257_1, had the same linear PS precursor as the star copolymers 167_6-148_6, 167_6-282_6, and 167_6-365_6 and will be used as a reference for our morphological study.

In as-cast films from solutions in chloroform of sample 180_6-65_6, no phase separation is visible, suggesting that both types of arms are in a mixed state. This nonequilibrium state is due to the short length of the P2VP blocks (the system is close to the order−disorder transition) as well as to the fact that mixing of the blocks is facilitated by the use of a common good solvent for PS and P2VP.[39,40] For all other samples, rapid casting from solutions in chloroform results in a lamellar morphology (Figure 2). Upon annealing, we should observe either an evolution of the period of the lamellae toward the equilibrium size or a transition from lamellae to cylinders or spheres. Such a transition, which requires only the splitting of the lamellae into objects of smaller size but different geometry, should happen relatively easily, as it would involve no coalescing process.[41]

3.1. Phase Diagram. The star copolymers that we consider are of the A_nB_n type. According to both theoretical studies of Olvera de la Cruz et al.[33] and Milner,[34] the χN_0 vs ϕ_{PS} phase diagram should in this case be very similar to that of linear diblock copolymers. Schulz et al.[42] have studied the phase behavior of PS−P2VP diblock copolymers in range of χN_0 up to 30 and for compositions ranging from $\phi_{PS} = 0.35$ to 0.70. Existence of a stable lamellar phase was observed between $\phi_{PS} = 0.40$ and 0.63. Cylindrical morphology has appeared at $\phi_{PS} = 0.35$ and $\phi_{PS} = 0.70$, while more complex bicontinuous structures are susceptible to appear for $0.35 < \phi_{PS} < 0.40$ and $0.63 < \phi_{PS} < 0.70$. Surprisingly this phase diagram exhibits a certain asymmetry around Φ_{PS} although there is a conformational resemblance between the two repeat units. Indeed the $l = V/R_g^2$ parameters of Milner's theory[34] for both PS and P2VP are quite similar since the flexibility of the PS and P2VP chains are nearly identical. The values of χN_0 calculated for our five PS_nP2VP_n stars are given in Table 2. These values are between 25 and 60, which corresponds to the intermediate segregation regime treated by Matsen et al.[43] for diblock copolymers (Figure 3). Therefore, it seems reasonable to compare our results with this theoretical phase diagram as well as with the experimental phase diagram established by Schulz et al.[42]

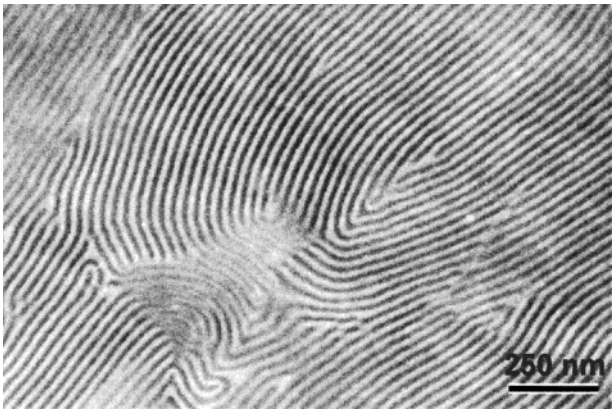

Figure 2. TEM micrograph of sample 205_6-240_6 ($\phi_{PS} = 0.48$) as-cast from a solution in chloroform, showing a lamellar morphology.

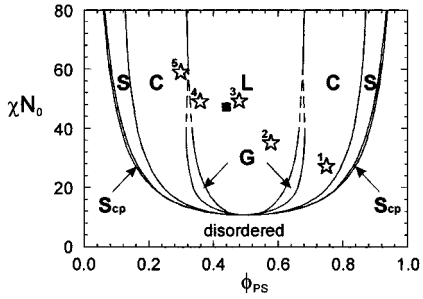

Figure 3. Theoretical phase diagram calculated by Matsen et al.[43] for diblock copolymers in the intermediate segregation regime. The positions of the five PS_6P2VP_6 samples on this phase diagram are denoted by the star symbols (☆). The numbering corresponds to the following: **1**, 180_6-65_6; **2**, 167_6-148_6; **3**, 205_6-240_6; **4**, 167_6-282_6; **5**, 167_6-365_6. Diblock copolymer 167_1-257_1 is indicated by a square symbol (■).

TEM micrographs of cross-sectional views of the five PS_nP2VP_n samples annealed for 17 h are shown in Figure 4, parts a−e. The three samples 167_6-148_6, 205_6-240_6, and 167_6-282_6 (Figure 4, parts b−d) with volume fractions of PS of 0.36, 0.48, and 0.58, respectively, exhibit stable lamellar morphologies. Upon annealing of the as-cast specimens, we observe an increase in the lamellar period up to 27, 35, and 37 nm, respectively. If we look at the position of these samples on theoretical phase diagram for diblock copolymers by Matsen et al.[43] (stars 2, 3, and 4 in Figure 3), we see that, according to the volume fraction of PS, all three samples lie in the region of stability of the lamellar

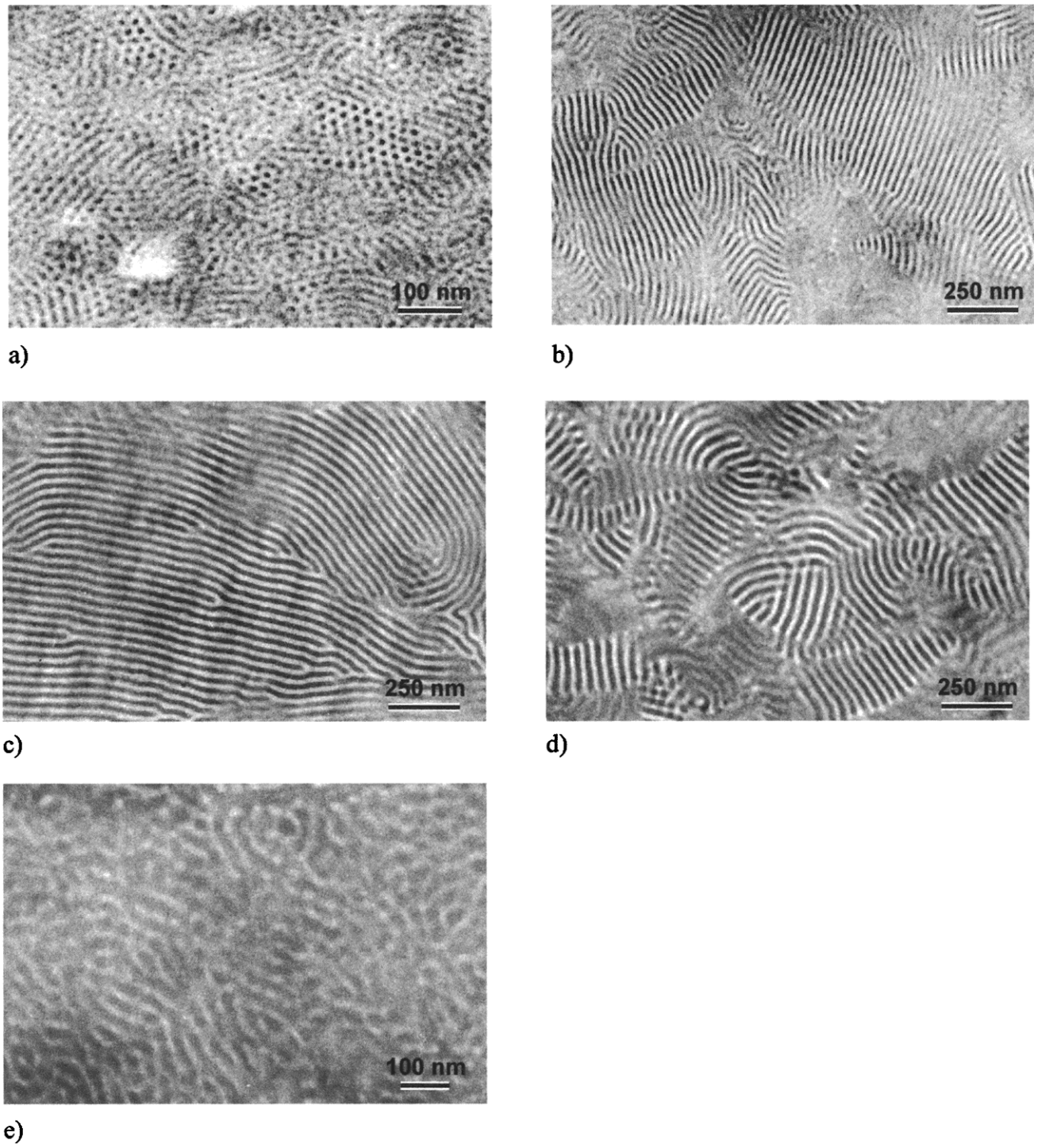

Figure 4. TEM micrographs of PS_6P2VP_6 heteroarm star copolymers cast from chloroform and annealed for 17 h at 160 °C: (a) 180_6-65_6; (b) 167_6-148_6; (c) 205_6-240_6; (d) 167_6-282_6; (e) 167_6-365_6.

phase. However, we note that the lamellar morphology of the sample 167_6-282_6 (star 4 in the phase diagram) is different from the cylindrical structure observed for a PS−P2VP diblock copolymer with the same PS volume fraction ($\Phi_{PS} = 0.35$).[42] In principle, this discrepancy could be attributed to the uncertainty on the determination of the position on the phase diagram (i.e., the error on the determination of the molecular characteristics may reach 10%). However, it is more likely that for heteroarm star copolymers, the crowding around the central junction point of the star block copolymers hinders the bending of the interface so that the stability of the lamellar phase might extend beyond the lamellae/cylinder phase boundary observed for diblock copolymers.

For sample 167_6-365_6 ($\phi_{PS} = 0.30$), a cylindrical structure might also be expected (star 5 in Figure 3) but is not observed experimentally (Figure 4e). The images obtained do not allow the precise identification of the structure. We observe that darker P2VP channels appear in the PS phase connecting the preexisting P2VP lamellae and inversely, lighter PS channels appear in the P2VP phase. Moreover, no particular ordering of the microdomains is observed. The morphology observed

Table 3. Comparison between Experimental and Theoretical Values of the Lamellar Period of Symmetrical "High" Functionality Heteroarm Star Copolymers − Dimensions of the Interfacial Region of Mixing

sample[(ref)]	N_0	f	L_{exp}(nm)	L_{dib}[b] (nm)	$\|1 - L_{dib}/L_{exp}\|$	R_0/R	V_0 (nm^3)	L_{th}[c](nm)	$\|1 - L_{th}/L_{exp}\|$
167_6-148_6	315	13.8	27	22.4	0.17	0.12	10.4	28.3	0.05
205_6-240_6	445	12.6	35	28.2	0.19	0.10	9.0	35.0	>0.01
167_6-282_6	449	13.8	37	28.4	0.23	0.10	10.4	35.7	0.04
VS1[(28)a]	470	16.1	37.1	26.7	0.28	0.10	11.8	35.9	0.03
VS2[(28)a]	1069	15.5	51.5	46.1	0.10	0.06	11.2	61.3	0.16
VS3[(28)a]	1404	15.6	64.1	54.9	0.14	0.06	11.3	73.1	0.12

[a] PS_8PI_8, "vergina" heteroarm star copolymers [b] Lamellar periods calculated using $L = cN_0^{2/3}$ scaling law: (i) for PS_nP2VP_n stars $c = L_{ref}/N_{ref}^{2/3}$, where L_{ref} and N_{ref} correspond to the reference diblock copolymer 167_1-257_1; (ii) for PS_nPI_n stars, $c = 0.44$, according to ref 47. [c] Lamellar periods calculated from eq 12.

might be a sort of "bicontinuous" structure (with average microdomain size of about 40 nm) or just a nonequilibrium kinetically frozen state. This result can be attributed to the following factors: (i) the composition of the sample corresponds to a point on the phase diagram (star 5 in Figure 3), which is very close to the boundary of lamellae/cylinders phase transition, and in this region the appearance of a metastable "bicontinuous/disordered" phase could come as no surprise even for diblock copolymers; (ii) the sample is the one with the highest molecular weight. This factor added to the star architecture of the molecules can be responsible for a considerable increase in the relaxation (reequilibration) time needed for this sample. Existence of a disordered equilibrium structure has been already observed by Pochan et al.[25,26] for a 2:1 PI/PS Y-shaped simple graft copolymer. These authors observed that for a composition of 0.81 volume fraction of PS, which lies at the boundary between bicontinuous and cylindrical phase in Milner's phase diagram, no ordered structure can be found. The equilibrium morphology is presumably the so-called randomly oriented wormlike micelles (ROW phase).[25,26]

For both samples 167_6-282_6 ($\phi_{PS} = 0.36$) and 167_6-365_6 ($\phi_{PS} = 0.30$), the observed morphology is strongly influenced by the molecular architecture. The penalty for blocks (star arms) bending at the interface is naturally larger for heteroarm stars than for diblocks so that all the phase transition boundaries are shifted toward more asymmetrical compositions.

Sample 180_6-65_6 ($\phi_{PS} = 0.75$) shows after annealing a structure made of small regions of hexagonally packed P2VP cylinders with a spacing of 20 nm (Figure 4a). This observation is in agreement with the expectations originating from both theoretical (star 1 in Figure 3) and experimental phase diagrams for PS−P2VP diblock copolymers. A summary of these results is given in Table 2.

3.2. The Influence of the Star Functionality on the Period of the Lamellae. It is known that, for diblock copolymers, the size of the domains depends mainly on the length of the blocks: it scales as $N^{1/2}$ in the weak segregation limit (WSL) and as $N^{2/3}$ in the strong segregation limit (SSL). For heteroarm star copolymers with equal number of A and B arms, one can expect the size of the domains to be dependent on N_0, the total number of segments in one A plus one B branch. Calculations in the WSL predict the domains to be smaller than that of a comparable diblock copolymer.[33] In the SSL, the impact of star architecture is reduced to a very tiny region around the interface and does not influence significantly the size of the domains. Most experimental studies deal with samples of $\chi N_0 \sim 40-100$.[21,22,25−30,32] In this regime, no general trend of the influence of the architecture of heteroarm stars on the domain size has been observed. Ishizu et al.[21] report about cylindrical structures from two PS−PI heteroarm star copolymers with mean functionality of ∼8 and 6 where the measured radii of the PI cylinders are significantly smaller than for diblock copolymers. In other studies,[27,30] the sizes measured are larger or comparable to that of equivalent diblock copolymer. It is of importance to note that those latter studies are dealing with samples with different number of arms of the two blocks. In our case, however, we are restricted to A_nB_n type heteroarm star copolymers with equal number n of A and B arms.

The periods of the equilibrium structures formed by our samples after annealing are collected in Table 2.[44] It is worthwhile to compare the results obtained for heteroarm star copolymers with that for the conventional diblock copolymers. For the sake of simplicity we will only consider the samples forming stable lamellar structures (relative volume fraction $\phi \sim 0.35-0.65$). For samples 167_6-148_6, 205_6-240_6 and 167_6-282_6, we calculated the values of the periods expected for diblock copolymers with identical degrees of polymerization of the blocks using a $N_0^{2/3}$ dependence. These values are given in Table 3 (L_{dib}) together with their deviation from the experimentally measured periods of the stars.

From the data present in Tables 2 and 3, it is clear that in the range of arm lengths considered, the PS_6-$P2VP_6$ heteroarm stars show a significant increase in the lamellar thickness. We can compare directly the diblock 167_1-257_1 with the star 205_6-240_6, which has very similar relative volume fraction and arm lengths. We see that a considerable increase in the thickness of the lamellae, from 27 nm for the diblock copolymer (Table 2) to 35 nm for the star, takes place. This corresponds to about 25% increase for the period. In a similar way, for the star 167_6-148_6 which has a similar PS arm length but a ∼40% shorter P2VP block length than the diblock 167_1-257_1, the value of the period 27 nm has been observed. This is exactly the same value of the period as for the diblock copolymer 167_1-257_1 (Table 2). The value of the period observed for the heteroarm star copolymer is in fact ∼20% higher than the value expected for the diblock copolymer of similar composition and block length, ∼22 nm (using $N^{2/3}$ dependence, Table 3). The third star 167_6-282_6 also provides a value of the period of 37 nm, which is considerably larger than the value expected for the reference diblock copolymer (28 nm).

Similar observations have been made for the PS_8PI_8 "vergina" stars studied by Beyer et al.[28] with a mean functionality of 16 (Table 3). A 12−39% increase in the value for the period of structures formed by heteroarm star copolymer compared to diblock copolymers of similar block length has been reported. Even for a functionality of four as for a PS_2PB_2 sample, Turner et

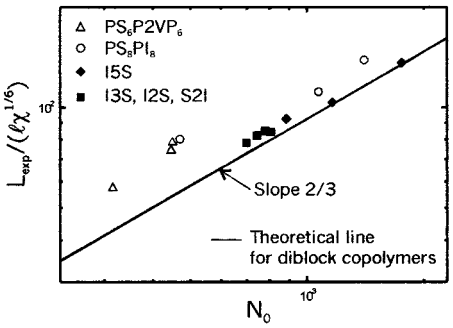

Figure 5. A log−log plot of $L_{exp}/(l\chi^{1/6})$ vs N_0 for heteroarm star copolymers. The solid line corresponds to the $N_0^{2/3}$ scaling of diblock copolymers.

Table 4. Comparison between Experimental and Theoretical Values of the Lamellar Period of Asymmetrical "Low" Functionality Heteroarm Star Copolymers: Dimensions of the Interfacial Region of Mixing

sample[ref.]	N_0	ϕ_{PS}	f	L_{exp} (nm)	L_{dib}[a] (nm)	R_0/R	V_0 (nm^3)	L_{th}[b] (nm)
S2I-49[27]	697	0.51	3	36.1	33.5	0.05	0.7	37.2
I2S-3[25]	806	0.62	3	39.0	36.9	0.05	0.8	38.9
I3S-55[27]	779	0.55	4	39.2	36.0	0.05	1.0	38.5
I3S-61[27]	742	0.61	4	38.0	34.9	0.05	1.0	37.0
I5S-1[32]	884	0.60	6	42.7	39.2	0.06	1.5	41.5
I5S-2[32]	1162	0.67	6	47.9	47.0	0.06	1.5	48.6
I5S-3[32]	1753	0.77	6	62.9	61.9	0.06	1.6	62.2

[a] Lamellar periods calculated using a $N_0^{2/3}$ scaling law, taking as reference experimental values of L for PS−PI diblock copolymers from ref 47. [b] Lamellar periods calculated from eq 15.

al.[30] found a discrepancy of ∼7% between a heteroarm star copolymer and a comparable diblock copolymer.

As is seen from Figure 5, where the dependence of $L/(l\chi^{1/6})$ on $N_0^{2/3}$ is presented, the deviation from the $N_0^{2/3}$ scaling law obeyed by diblock copolymers is especially pronounced for the PS_6P2VP_6 samples as well as for the PS_8PI_8 heteroarm star VS1, all samples with arm lengths resulting in $N_0 \sim 400-500$. Since the deviation is observed for stars of different chemical natures, this seems to be a general trend. Even for asymmetric stars of low functionality[25,27,32] listed in Table 4, there is some deviation from the $N_0^{2/3}$ scaling law (Figure 5) when N_0 is not too large. As is seen from Figure 5 and Tables 3 and 4 the deviation from $N_0^{2/3}$ dependence for asymmetric stars is considerably smaller than that for symmetric ones, but still has a systematic character: the value of the lamella period experimentally observed is always larger than the value predicted for the corresponding diblock copolymers. For star molecules of higher arm length (VS2, VS3), the deviation is still present but less pronounced. For I_5S-2, I_5S-3 with $N_0 > 10^3$, the deviation becomes indistinguishably small both because of large arm length and low functionality of the stars (Figure 5). Thus, it seems that for heteroarm stars the peculiar architecture of the molecules influences greatly the domain sizes of the microphase separated morphologies especially in the region of an "intermediate arm length", where $N_0 \sim 400-500$ ($N_0 < 10^3$). Furthermore, for a given value of N_0, the larger the functionality of stars, the larger is the deviation from the $N_0^{2/3}$ scaling law for conventional diblock copolymer. This implies that the presence of multiple junction point induces a much more compact brush at the interphase than in the case of diblock copolymers. Consequently, an additional stretching of the arms of the star copolymer (compared to diblock copolymers) occurs near the interface, leading to the increase in the period of the structure. This effect naturally diminishes with decreasing star functionality or when the length of the arms becomes sufficiently large to screen the effect of conformational peculiarities at the interface.

3.3. Theoretical Model. As is discussed previously, neither the existing models for diblock copolymers nor the modified model proposed by Beyer et al.[28] to fit experimental data is adequate to describe the self-assembling properties of heteroarm stars. Therefore, further attempts to construct a relevant model are required. To this end, let us first analyze what physical reason makes the behavior of heteroarm stars forming lamellar layers different from that of diblock copolymers. The reason lies naturally in the molecular architecture. The difference is in the way the two sets of blocks of different chemical nature are linked together. For diblock copolymers, the "single" junction points delimit the different layers. In the vicinity of the interface, the unfavorable contacts between blocks induce the stretching of both A and B blocks in the direction perpendicular to the interface. In the case of heteroarm stars, the junction points are also located at the interface where stretching of the arms also occurs, but the "multiple" junction points prevent the arms from assuming their preferable orientation perpendicular to the interface. This results in an additional chain stretching near the interface. Indeed, the conformation of the arm tails of heteroarm stars copolymers and diblock copolymers far away from the lamellar interface is nearly independent of the conformation of the part of the chain near the interface due to the screening effect. Hence, the main difference in the lamellar spacing is expected to be due to the region near the interface. The chain stretching for heteroarm star copolymers near the interface will be considerably larger than in the case of diblock copolymers leading to the increase of lamellar spacing.

The conformation of the blocks near the junction point has a lot of common features with that described by the Daoud−Cotton model for star homopolymers.[45] However there is one significant difference: the arms have to deviate from their original radial trajectory in order to reach the half-space of the lamella formed by the blocks of similar chemical nature (Figure 6a). As a consequence, there is an interfacial volume around the junction point, where monomer units of both blocks are mixed, and where the main interaction between the blocks occurs, as has been evidenced experimentally.[20] Outside this region the concentration of one or the other sort of blocks is dominant. The free energy of volume interactions per molecule inside the region of mixing is[46]

$$F_{int} = \int \chi\phi(1-\phi)\, dV/v = \chi \frac{1}{4}\frac{V_0}{v} \qquad (1)$$

where V_0 is the volume of the interfacial mixing area and v is the volume per monomer (e.g., for definiteness of sort B, $v \equiv v_B$). In eq 1, we assume that the volume fractions of both blocks inside this region are equal, which is strictly correct only for stars with an equal number of A and B arms. For strongly asymmetric stars, some modification may be needed, as we will discuss below.

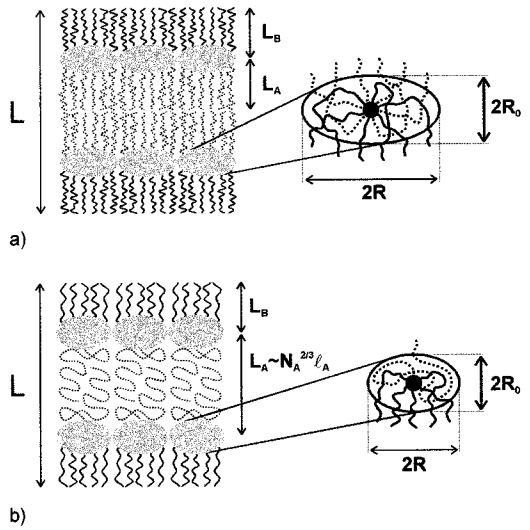

Figure 6. Schematic representation of the conformation of the heteroarm star copolymers forming lamellar structures: (a) symmetric heteroarm stars with relatively high functionality: (b) asymmetric heteroarm stars with one A arm and several B arms. (Due to the large difference in lengths of A and B blocks, there are reasons (supported by experimental evidence) to believe that each A arm extends almost inside the entire layer, so that the thickness of the layer formed by the A blocks scales as $N_A^{2/3}$.) Near the junction point, the segments of different chemical natures are mixed inside a symmetric oblate ellipsoid with radius R lying in the interfacial plane and radius $R_0 \leq R$ in the direction perpendicular to the interface.

Because of the spherical symmetry of the star molecules, it is natural to assume that this region near the junction point also has a spherical shape (especially for symmetric stars). However, the symmetry with respect to the interface has also to be taken into account. The most general and realistic assumption corresponds to an oblate ellipsoid with two identical radii, equal to R, lying in the interface plane and with a radius $R_0 \leq R$ in the direction perpendicular to the surface (Figure 6a). Then, the interaction free energy assumes the form

$$F_{int} = \pi R^2 R_0 \chi/(3v) \tag{2}$$

When $R_0 \sim R$, which we would expect for the stars with high functionality and not-too-long arm length, the region of volume interactions is spherelike and the difference in the lamellar period between heteroarm star and diblock copolymers will be maximal. In the opposite limit, $R_0 \ll R$, which we can expect for stars with very long arms, the region of interactions between the monomers of different chemical nature is disklike, and the difference in lamellae structure for the stars and the diblock copolymers will be minimal. It is necessary to note that, in the latter case, the surface tension coefficient, rather than the χ-parameter, should be employed to characterize the interactions, and F_{int} should be written in a different form. In this paper, however, we will be mainly interested in cases where the star architecture essentially influences the lamellar structure.

The elastic free energy of heteroarm stars forming lamellae, describing the entropy loss per blocks stretching, can be split into two parts. The first cause of chain stretching is the presence of the planar interface between layers formed by different blocks. The corresponding free energy (which is similar to the diblock copolymer case[46]) is

$$F_{el} = \frac{\pi^2}{24}\left(f_A \frac{L_A^3}{N_A^2 v_A} + f_B \frac{L_B^3}{N_B^2 v_B}\right) \tag{3}$$

where, f_I, N_I and v_I are the functionality, chain length, and volume per monomer of an arm of sort I = A or B. L_A (L_B) is the radius of gyration of A (B) block, which is equal to half of the corresponding layer width.

Besides the stretching due to the lamellar layer structure, there is an additional local stretching of the arms near the junction point (around the ellipsoid), which is specific to the star molecules. This stretching is similar to what takes place in polymeric micelles in the vicinity of the surface of a micelle core.[46] It is possible to write the explicit expression for the corresponding energy of block stretching near an elliptic surface using an electrostatic analogy, however such exactness would make further calculations complicated without changing the final scaling laws. So, for the sake of simplicity in describing chain stretching near the junction point we will replace an ellipsoid by the sphere of the same volume $4\pi(R^*)^3/3$, where $R^* = R^{2/3}R_0^{1/3}$. The free energy accounting for the local stretching of all arms near the junction point can be written in the form

$$F_{loc} \cong \frac{3}{8\pi}\frac{v_A}{l_A^2}\frac{ff_A}{R^*} + \frac{3}{8\pi}\frac{v_B}{l_B^2}\frac{ff_B}{R^*} \tag{4}$$

where the total "charge" ("aggregation number") of the ellipsoid (sphere) is equal to f and l_A and l_B are the monomer lengths of arms of types A and B, respectively.

Taking into account the incompressibility conditions

$$\pi R^2 L_A = f_A N_A v_A$$
$$\pi R^2 L_B = f_B N_B v_B \tag{5}$$

the radius R and the radius of gyration L_A of the A block in lamellae can be expressed via L_B.

$$L_A = L_B \frac{f_A N_A v_A}{f_B N_B v_B} \tag{6}$$

Then the free energy per molecule forming a lamella can be presented in the form

$$F = \frac{f_B N_B}{3L_B} R_0 \chi + \frac{3}{8\pi} S \frac{f_B^{5/3}}{l_B^2}\left(\frac{L_B}{R_0}\right)^{1/3}\left(\frac{\pi v_B^2}{N_B}\right)^{1/3}\left(1 + \frac{f_A}{f_B}\right) + \frac{\pi^2}{24} f_B \frac{L_B^3}{N_B^2 v_B} Y \tag{7}$$

where

$$S = 1 + \frac{v_A}{v_B}\left(\frac{l_B}{l_A}\right)^2 \frac{f_A}{f_B} \tag{8}$$

$$Y = 1 + \left(\frac{f_A}{f_B}\right)^4 \left(\frac{v_A}{v_B}\right)^2 \frac{N_A}{N_B} \tag{9}$$

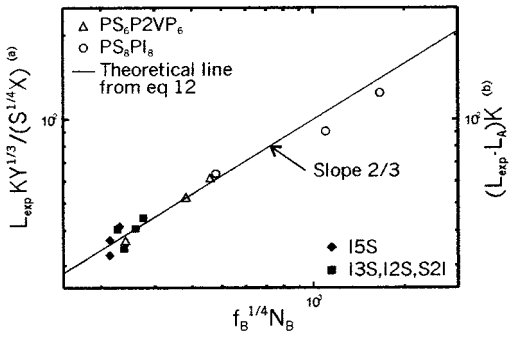

Figure 7. A log−log plot of the lamellar period vs $f_B^{1/4}N_B$, for (a) symmetric (open symbols, left vertical axis) and (b) asymmetric (solid symbols, right vertical axis) heteroarm star copolymers. The parameter K is defined by eq 14. For asymmetric stars, the thickness of the A layer is approximated by the formula $L_A \cong 0.82 l_A \chi^{1/6} N_A^{2/3}$. The two families of samples can be fitted with the same line of slope $= {}^2/_3$ as predicted by our theoretical model (eqs 12 and 15).

The free energy actually depends only on two independent variables, R_0 and L_B. To obtain the equilibrium values of R_0 and L_B, the free energy per unit volume

$$\mathbf{F} = \frac{F}{V_1} \qquad V_1 = L_A f_A + L_B f_B \tag{10}$$

should be minimized. As a result of minimization, the following expressions for the radius R_0 and the period of lamellar structure $L_{th} = 2(L_A + L_B)$ are obtained

$$R_0 \cong \left(\frac{3}{8}\right)^{3/4} \frac{1}{\pi^{1/2}} \frac{f_B^{1/2} L_B}{N_B} \frac{\nu_B^{1/2} S^{3/4}}{l_B^{3/2} \chi^{3/4}} \left(1 + \frac{f_A}{f_B}\right)^{3/4} \tag{11}$$

$$L_{th} \cong C f_B^{1/6} N_B^{2/3} \chi^{1/12} \frac{\nu_B^{1/2}}{l_B^{1/2}} \frac{S^{1/4}}{Y^{1/3}} \left(1 + \frac{f_A}{f_B}\right)^{1/4} X = f_B^{1/6} N_B^{2/3} \frac{S^{1/4}}{K Y^{1/3}} X \tag{12}$$

where C is a numerical coefficient ($C \sim 0.78$), S and Y are defined by eqs 8 and 9, and

$$X = 1 + \frac{f_A N_A \nu_A}{f_B N_B \nu_B} \tag{13}$$

$$K = \frac{1}{C} \frac{l_B^{1/2}}{\chi^{1/12} \nu_B^{1/2}} \left(1 + \frac{f_A}{f_B}\right)^{-1/4} \tag{14}$$

As can be seen from Table 3, where the ratio of R_0/R is presented, our initial assumption about an oblate shape of ellipsoid (i.e., $R_0/R < 1$) is correct. For the four symmetric stars with $N_0 \sim 500$, i.e., for all the three PS_6P2VP_6 samples and VS1, this ratio is about 0.1. It becomes smaller (∼0.06) for stars with longer arm lengths (VS2, VS3) as we expected.

The dependence of $L_{exp}KY^{1/3}/(S^{1/4}X)$ for symmetric stars on $f_B^{1/4}N_B$ is presented in logarithmic scale in Figure 7. The product $L_{exp}KY^{1/3}/(S^{1/4}X)$ differs from the experimentally measured lamellar period L_{exp} only by the numerical coefficient depending on particular star composition (f_A, f_B) and conformation (l_A, l_B, ν, χ). In contrast to Figure 5 not only the dependence on block length, but also on star functionality is analyzed in Figure 7. As we see all the PS_6P2VP_6 samples forming lamellar structure (open triangles) as well as the PS_8-PI_8 stars samples studied by Beyer[28] (open circles) can be fitted nicely by the linear dependence with the slope equal to ${}^2/_3$, which exactly corresponds to the theoretical prediction of eq 12. Hence, the additional chain stretching near the multiple junction point (i.e., in the vicinity of the ellipsoid of volume interactions), which was the main factor considered in our model in addition to "ordinary" chain stretching, does play an important role in the determination of the equilibrium lamellar period, at least for the stars with chain lengths considered experimentally. We note, however, that the agreement is somewhat worse for the stars with long arm length (VS2, VS3) for which our model gives somewhat overestimated values. The reason is the form of interaction free energy applied (eq 2), as we discussed above. Indeed, our model takes into account mainly the volume interactions (between monomers of different chemical nature situated near the junction point) that play the dominant role for the stars with not-too-long arm length. In fact, there might also be some surface interactions if the arms spread out along the interface. Such surface interactions are counted in our model in indirect way as some averaged contribution to the overall interaction. For the stars with long arm length, surface interactions seem to be equally important as volume interactions and in this way our model apparently overestimate the overall monomer interaction providing larger value for the lamellar period compared to experimental observations. Diblock copolymer model as applied to stars, on the contrary, gives underestimated prediction for the period (Figure 5) neglecting the volume interactions at all. So, we expect our model to work the best for the stars (of high functionality) with small to intermediate arm length (Figure 7) for which the volume interactions near the junction point are of primarily importance, leading to the most pronounced difference between experimental results and predictions of diblock copolymer model (Figure 5).

Numerical comparisons of the values for the lamellar period measured experimentally and calculated analytically using the eq 12 are presented in Table 3. It is evident that, practically in all cases (except for long arm stars VS2 and VS3), the present model gives considerably better prediction of the lamellar period for all stars compared to the estimation provided by the diblock copolymer model (cf. also Figures 5 and 7). This proves again that molecular architecture plays an important role in microphase separation of polymer systems and the predictions made for one polymer system may not work well for the other.

Now, there are also experimental data regarding asymmetric ($f_A \neq f_B$) heteroarm stars of low functionality from refs 25, 27, and 32. For these samples, the diblock copolymer model still seems to work reasonably well, however with a systematic deviation: experimentally measured periods of all stars are always larger than the values predicted for the conventional diblock copolymers. Can our model predict correctly the lamellar spacing for these samples as well? For all these samples, the stars are constituted of one single arm of one of the species, which we will refer to as polymer A, and several arms (two to five) of the other species (B). Because the architectural asymmetry is rather strong, we cannot expect any extra stretching of the single A block near the interface compared to the diblock copoly-

mer case, so that the direct substitution of the experimental data for asymmetric stars into eqs 11 and 12 is impossible. Since the volume fraction of the A-block is comparable with that of f_B B blocks (i.e., the length of an A block is considerably larger than that of a B block), the A block may actually fill nearly the whole width of the A layer (Figure 6b). The analysis of experimental data seems to support this assumption: the best fit of experimental data (based on this hypothesis) gives us $L_A \cong 0.82 l_A \chi^{1/6} N_A^{2/3}$, which is very close to the standard scaling law for diblock copolymers as to be expected for the A block. As to B blocks, they will be extra-stretched near the interface due to the presence of the multiple junction point similar to the case of symmetric stars. We can repeat all the analytical considerations described above making only one correction: L_A is now a known value from the very beginning. As a result, we will have the same expression for R_0 as in eq 11, only now $S \sim 1$. Again, we find that for all the asymmetric samples $R_0/R < 1$. Moreover, the volume of the ellipsoid V_0 (i.e., the volume where the interactions between A and B monomers occurs) turns out to be smaller for asymmetric stars compared to symmetric ones, as one could expect (Table 4). Indeed, for asymmetric stars containing only one A block, A and B blocks can be easily disentangled near the interface, so that only few monomers per B block have a contact with A monomers.

For the period of lamellae L of asymmetric stars we get

$$L_{th}^{as} \cong L_A + C f_B^{1/6} N_B^{2/3} \chi^{1/12} \frac{\nu_B^{1/2}}{l_B^{1/2}} \left(1 + \frac{f_A}{f_B}\right)^{1/4} = L_A + \frac{f_B^{1/6} N_B^{2/3}}{K} \quad (15)$$

As is seen from eq 15 the power dependence of L_{th}^{as} on $f_B^{1/4} N_B$ is practically the same as for symmetric stars, except for the prefactor and the additional term, L_A. This difference reflects the difference in chain architecture resulting in different chain conformations near the interface and inside the layers. We plotted $(L_{exp} - L_A)K$ (which is related to the experimentally observed width of lamellar layer formed by a B block) for asymmetric stars vs $f_B^{1/4} N_B$ in logarithmic scale in the same Figure 7 as for symmetric stars. We found that B-layer spacing for asymmetric stars follows the same dependence as the period for symmetric stars. All points for asymmetric stars can be well fitted by the scaling law described by eq 15. The quantitative comparison of the experimental data and the theoretical results for the period of lamellae for asymmetric stars is presented in Table 4. As it follows from the Table, the theoretical values for the period of asymmetric stars provided by the present model are even somewhat closer to the experimental values than that obtained in the framework of diblock copolymer model. However, the difference between the two models is not so pronounced as for symmetric stars of larger functionality. Nevertheless, the predictions of the present model are free of any systematic deviations to larger or smaller side in contrast to the diblock copolymer model (cf. Figures 5 and 7). Hence, the present model proves to be successful in both predicting the scaling laws and providing reasonably good numerical estimations for the lamellar period of both symmetric stars of large functionality and asymmetric stars of low functionality. This means that despite the fact that the conformations of A blocks for symmetric and asymmetric stars are different, in both cases there is an extra stretching of the B blocks (near the junction point, in the vicinity of the interface), which turns out to be a characteristic signature of heteroarm stars, making their self-assembly properties different from that of diblock copolymers.

This result together with observations for the phase diagram discussed above allow us to conclude that the usual opinion that heteroarm stars (or other polymers with complex architecture) can be treated as conventional block copolymers is not correct. If such a comparison is possible, it is only for the very long chains, when the chain architecture has less influence on the large-scale properties of structure. In all other cases, the peculiar chain conformation associated with the star architecture is of dominant importance for the microphase separation properties of these materials and the observed difference from the diblock copolymer case is the natural outcome of the difference in molecular architecture.

4. Conclusions

We have studied the phase behavior and association properties of a series of five PS_nP2VP_n heteroarm star copolymers. We have found that chain architecture plays an important role in the phase behavior. As a result, the equilibrium structures formed by heteroarm star copolymers often turned out to be different than that expected for conventional diblock copolymers or than what was predicted for heteroarm stars.[33,34] For instance, 167_6-365_6 sample, for which cylindrical structure was expected,[43] exhibits no easily identified ordered morphology. Some complex "bicontinuous" or "disordered" morphology is suspected. The reason for such behavior might be slow kinetics of equilibration attributed to the star architecture in combination with large length of arms. At the same time, four other samples did reach the equilibrium cylindrical (180_6-65_6) and lamellar (167_6-148_6, 205_6-240_6, and 167_6-282_6) structures.

In accordance with previous observations for heteroarm star copolymers,[27,28,30] the periods of lamellar structures formed by our samples are found to exceed the periods observed for conventional diblock copolymers by 20−30%. The analysis of available experimental data shows that this difference is the most pronounced for the stars of large functionality with block length varying from small to intermediate. For the stars with long arm length, the difference with the conventional diblock copolymers becomes smaller. We have shown that the physical reason for the increase in lamellar period is connected with the chain architecture, namely this is an extra stretching of blocks near the junction point in the vicinity of the interface. The proposed theoretical model takes into account the above-mentioned effect and predicts the increase of the period of lamellae for heteroarm star copolymers as the star functionality increases as $f^{1/6} N^{2/3} \chi^{1/12}$. The rate of the increase does depend on the block lengths (the proposed model works the best for the stars with small or intermediate arm length) and on the interaction parameter. The comparison of the theoretical predictions with our experimental data and other available data shows that remarkable agreement is achieved for both symmetric samples of large functionality and samples of low functionality with large architectural asymmetry.

Acknowledgment. Financial support from The Netherlands Organization for Scientific Research (NWO–CW, FOM) is gratefully acknowledged. C.T. would like to thank in particular the NWO for financial support for his stay at the University of Groningen. V.G. thanks the European Union for a grant within the "Marie Curie" TMR program. E.E.D. is also grateful to the MRSEC Program of the National Science Foundation under Award DMR-9809364 for financial support during the completion of this work.

References and Notes

(1) Alward, D. B.; Kinning, D. J.; Thomas, E. L.; Fetters, L. J. *Macromolecules* **1986**, *19*, 215.
(2) Tsitsilianis, C.; Chaumont, P.; Rempp, P. *Makromol. Chem.* **1990**, *191*, 2319.
(3) Tsitsilianis, C.; Graff, S.; Rempp, P. *Eur. Polym. J.* **1991**, *27*, 243.
(4) Kanaoka, S.; Omura, T.; Sawamoto, M.; Higashimura, T. *Macromolecules* **1992**, *25*, 6407.
(5) Iatrou, H.; Hadjichristidis, N. *Macromolecules* **1993**, *26*, 2479.
(6) Quirk, R. P.; Yoo, T.; Lee, B.*J. M. S. Pure Appl. Chem.* **1994**, *A31*, 911.
(7) Tsitsilianis, C.; Papanagopoulos, D.; Lutz, P. *Polymer* **1995**, *36*, 3745.
(8) Tsitsilianis, C.; Voulgaris, D. *J. Macromol. Sci.—Pure Appl. Chem. Macromol. Rep.* **1995**, *A32*, 569.
(9) Avgeropoulos, A.; Poulos, Y.; Hadjichristidis, N.; Roovers, J. *Macromolecules* **1996**, *29*, 6076.
(10) Allyaier, J.; Young, N.; Efstratiadis, Y.; Hadjichristidis, N. *Macromolecules* **1996**, *29*, 1794.
(11) Miyata, K.; Watanabe, Y.; Itaya, T.; Tamigaki, T.; Inoue, K. *Macromolecules* **1996**, *29*, 3694.
(12) Hadjichristidis, N.; Pispas, S.; Pitsikalis, M.; Iatrou, H.; Vlahos, C. *Adv. Polym. Sci.* **1999**, *142*, 71.
(13) Hadjichristidis, N. *J. Polym. Sci. Part A: Polym. Chem.* **1999**, *37*, 857.
(14) Fernyhough, C. M.; Young, R. N.; Tack, R. D. *Macromolecules* **1999**, *32*, 5760.
(15) These kind of polymers also are referred as "miktoarm" stars meaning stars with mixed arms. The term "heteroarm" renders precisely the A_nB_n architecture since these kind of star-shaped polymers bear chemically different pure arms.
(16) Tsitsilianis, C.; Kouli, O. *Macromol. Rapid. Commun.* **1995**, *16*, 591.
(17) Voulgaris, D.; Tsitsilianis, C.; Esselink, F. J.; Hadziioannou, G. *Polymer* **1998**, *39*, 6429.
(18) Pispas, S.; Poulos. Y.; Hadjichristidis, N. *Macromolecules* **1998**, *31*, 4181.
(19) Voulgaris, D.; Tsitsilianis, C.; Grayer, V.; Esselink, F. J.; Hadziioannou, G. *Polymer* **1999**, *40*, 5879.
(20) Tsitsilianis, C. *Macromolecules* **1993**, *26*, 2977.
(21) Ishizu, K.; Kuwahara, K. *Polymer* **1994**, *22*, 4907.
(22) Floudas, G.; Hadjichristidis, N.; Iatrou, H.; Pakoula, T.; Fischer, E. W. *Macromolecules* **1994**, *27*, 7735.
(23) Floudas, G.; Pispas, S.; Hadjichristidis, N.; Pakoula, T.; Erukhimovich, I. *Macromolecules* **1996**, *29*, 4142.
(24) Tselikas, Y.; Hadjichristidis, N.; Lescanec, R. L.; Honeker, C. C.; Wohlegemuth, M.; Thomas, E. L. *Macromolecules* **1996**, *29*, 3390.
(25) Pochan, D. J.; Gido, S. P.; Pispas, S.; Mays, J. W.; Ryan, A. J.; Fairclough, J. P. A.; Hamley, I. W.; Terrill, N. J. *Macromolecules* **1996**, *29*, 5091.
(26) Pochan, D. J.; Gido, S. P.; Pispas, S.; Mays, J. W. *Macromolecules* **1996**, *29*, 5099.
(27) Tselikas, Y.; Iatrou, H.; Hadjichristidis, N.; Liang, K. S.; Mohanty, K.; Lohse, D. J. *J. Chem. Phys.* **1996**, *105*, 2456.
(28) Beyer, F. L.; Gido, S. P.; Poulos, Y.; Avgeropoulos, A.; Hadjichristidis, N. *Macromolecules* **1997**, *30*, 2373.
(29) Lee, C.; Gido, S. P.; Pitsikalis, M.; Mays, J. W.; Tan, N. B.; Trevino, S. F.; Hadjichristidis, N.*Macromolecules* **1997**, *30*, 3738.
(30) Turner, C. M.; Sheller, N. B.; Foster, M. D.; Lee, B.; Corona-Galvan, S.; Quirk, R. P.; Annís, B.; Lin, J.-S. *Macromolecules* **1998**, *31*, 4372.
(31) Werts, M. P. L.; van der Vegte, E. W.; Grayer, V.; Esselink, E.; Tsitsilianis, C.; Hadziioannou, G. *Adv. Mater.* **1998**, *10*, 452.
(32) Beyer, F. L.; Gido, S. P.; Velis, G.; Hadjichristidis, N.; Beck Tan N. *Macromolecules* **1999**, *32*, 6604.
(33) Olvera de la Cruz, M.; Sanchez, I. C. *Macromolecules* **1986**, *19*, 2501.
(34) Milner, S. T. *Macromolecules* **1994**, *27*, 2333.
(35) Olmsted, P. D.; Milner, S. T. *Macromolecules* **1998**, *31*, 4011.
(36) Buzza, D. M. A.; Hamley, I. W.; Fzea, A. H.; Moniruzzaman, M.; Allgaier, J. B.; Young, R. N.; Olmsted, P. D.; McLeish, T. C. B. *Macromolecules* **1999**, *32*, 7483.
(37) Tsitsilianis, C.; Voulgaris, D. *Macromol. Chem. Phys.* **1997**, *198*, 997.
(38) Hadjichristidis, N.; Tselikas, Y.; Iatrou, H.; Efstratiadis, Y.; Avgeropoulos, A. *J. Macromol. Sci.—Pure Appl. Chem.* **1996**, *A33*, 1447.
(39) Christopoulou, V.; Papanagopoulos, D.; Dondos, A. *J. Polym. Sci., Part B: Polym. Phys.* **1999**, *37*, 1051.
(40) Dondos, A.; Christopoulou, V.; Papanagopoulos, D. *J. Polym. Sci., Part B: Polym. Phys.* **1999**, *37*, 379.
(41) Sakurai, S.; Kawada, H.; Hashimoto, T.; Fetters, L. J. *Macromolecules*, **1993**, *26*, 5796.
(42) Schulz, M. F.; Khandpur, A. K.; Bates, F. S.; Almdal, K.; Mortensen, K.; Hajduk, D.; Gruner, S. M. *Macromolecules* **1996**, *29*, 2857.
(43) Matsen, M. W.; Bates, F. S. *J. Chem. Phys.* **1997**, *106*, 2436.
(44) The estimations of the period of structure from TEM images might not be as precise as that obtained by SAXS. We estimate the uncertainty (including the possible effect of staining) to be less than 5% of the values obtained. This uncertainty, however, does not influence seriously the results, which are consistent with the other experimental data (see Figure 5) (also obtained using SAXS). The characteristic deviations from the $N^{2/3}$ law considered in Figure 5 are considerably larger than the uncertainty in the value of the lamella period.
(45) Daoud, M.; Cotton, J. C. *J. Phys.* **1982**, *43*, 531.
(46) Semenov, A. N. *Sov. Phys. JETP* **1985**, *61*, 733.
(47) Hashimoto, T.; Fujimura, M.; Kawai, H. *Macromolecules* **1980**, *13*, 1660.

MA000311U